Time-dependent recovery of passive neutrophils after large deformation

R. Tran-Son-Tay, D. Needham, A. Yeung,* and R. M. Hochmuth
Department of Mechanical Engineering and Materials Science, Duke University, Durham, North Carolina 27706 USA, and
*University of British Columbia, Departments of Pathology and Physics, Vancouver, British Columbia, V6T 1W5 Canada

ABSTRACT Experiments are performed in which a passive human neutrophil is deformed into an elongated "sausage" shape by aspirating it into a small glass pipette. When expelled from the pipette the neutrophil recovers its natural spherical shape in ~1 minute. This recovery process is analyzed according to a Newtonian, liquid-drop model in which a variational method is used to simultaneously solve the hydrodynamic equations for low Reynolds-number flow and the equations for membrane equilibrium with a constant membrane tension. The theoretical model gives a good fit to the experimental data for a ratio of membrane cortical tension to cytoplasmic viscosity of $\sim 1.7 \times 10^{-5}$ cm/s (0.17 μm/s). However, when the cell is held in the pipette for only a short time period of 5 s or less, and then expelled, the cell undergoes an initial, rapid elastic rebound suggesting that the cell behaves in this instance as a Maxwell viscoelastic liquid rather than a Newtonian liquid with constant cortical tension.

INTRODUCTION

The ability of the neutrophil to deform and flow in capillaries and the ability to migrate in tissue is largely influenced by its mechanical properties. Passive neutrophils exhibit viscoelastic properties, which are essentially liquidlike in character during slow rates of deformation and elasticlike during rapid rates of deformation. These mechanical properties depend on the underlying structure of the cell and the organization of the structural components in the cellular cytoplasm and membrane cortex. One of these structural components, F-actin, undergoes local rearrangement during cell "activation" in response to a variety of stimuli, and thus the mechanical properties of the neutrophil are also very sensitive to its state of activation. In this paper, we are concerned with a mechanical description of the "passive" neutrophil in a resting, receptive state. In our experiments, this state is defined visually by a spherical appearance and the absence of lamellapodia (Needham et al., 1989).

The mechanical description of the passive neutrophil has been a focus of research in several laboratories in recent years. Much of this work has used the technique of micropipette manipulation to deform individual cells by well-characterized forces. The results from micromanipulation experiments that measure the entry and flow of single neutrophils into suction micropipettes have prompted the development of parameterized models of the cell. These models interpret static and time dependent cellular deformations in terms of linear arrangements of representative mechanical elements situated in the cytoplasmic interior and plasma membrane (Fig. 1).

The first of these models viewed the cell as a standard solid (Bagge et al., 1977; Schmid-Schönbein et al., 1981; Sung et al., 1988). As shown in Fig. 1 *a*, this early solid model has an elastic "Hookean" element in parallel with a Maxwell element. A Maxwell element consists of a spring or elastic component in series with a dashpot or viscous component. The experiments of Evans (1984), however, demonstrated that the neutrophil behaves less like a solid and more like a liquid drop (Fig. 1 *b*) and flows continuously into 3–6-μm capillary tubes as long as the aspiration pressure is sufficiently large so as to overcome a small "cortical tension" that exists in the surface or cortex of the passive neutrophil. It is this small cortical tension that causes the passive neutrophil to (eventually) assume a spherical shape after it has been deformed into some other, nonspherical geometry. Yeung and Evans (1989) and Evans and Yeung (1989) have recently shown that the cortex of the resting neutrophil has a small, persistent cortical tension of ~0.035 dyn/cm and that the cytoplasm, when modeled as a Newtonian liquid, has a large viscosity of 2,000 poise. An important finding of their work is that dissipation in the cortex is negligible in comparison to that in the bulk cytoplasm (i.e., the cortical surface viscosity is much less than the cytoplasmic viscosity multiplied by the cell radius).

Recently, we, and others, have observed that the cell behaves in an elastic manner when subjected to rapidly changing stresses such as would occur when the cell is aspirated rapidly into a small pipette or rapidly expelled from a tapered tube (Dong et al., 1988; Needham and

Address correspondence to Dr. Tran-Son-Tay.

0006-3495/91/10/856/11 $2.00

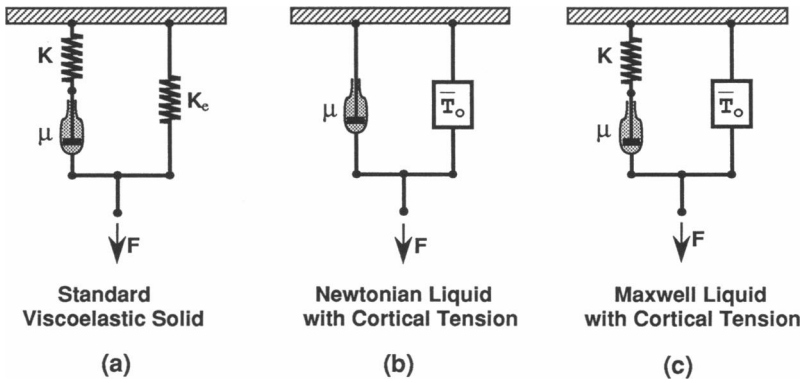

FIGURE 1 Parameterized models of the passive neutrophil. (**a**) Standard solid model (Bagge et al., 1977; Schmid-Schönbein et al., 1981). This early mode has an elastic "Hookean" element in parallel with a Maxwell element, and describes the cell in terms of three constants (two spring elements and a viscous element). (**b**) Liquid drop with cortical tension (Evans, 1984). Once the applied pressure exceeds the threshold pressure, determined by a persistent cortical tension, the cell flows into the pipette like a Newtonian liquid. (**c**) Maxwell fluid with cortical tension (Dong et al., 1988). The cell is represented as a prestressed cortical shell with a constant cortical tension in parallel with the cytoplasm, which behaves as a Maxwell fluid (i.e., Newtonian fluid with fading memory) characterized by a spring and a viscous element.

Hochmuth, 1990). This leads to the addition of another element to the Newtonian liquid drop model. The current model of the cell must therefore be viewed as a prestressed cortical shell with a constant cortical tension in parallel with the cytoplasm, which behaves as a Maxwell fluid (Fig. 1 *c*). Thus, the cell interior appears to be a highly viscous fluid with a fading elastic memory.

If the rheological models mentioned above are to have any validity, the numerical values for the various mechanical elements characterizing cell material properties must be constants and not functions of the extent and rate of deformation for a range of rheological tests. We are currently investigating the sensitivity of these models to experimental data. We are deriving values of the elastic and viscous components by performing a variety of experiments such as flow into a pipette, static deformation in a tapered tube, flow down a tapered tube and recovery after large deformation.

In the present paper, the validity of the Newtonian liquid model (Fig. 1 *b*) for the neutrophil in the recovery experiment, after large deformation, is investigated. For that particular purpose, the work is divided into two main parts: one experimental and one theoretical. In the first part, we report the results of experiments in which cells are deformed from their resting spherical geometry and released from this state and their progress of recovery is monitored. Holding times in the deformed state, before recovery is allowed to proceed, range from tenths of a second to tens of seconds. The presence of an "interior spring" element would suggest that the ability of the cell to recoil should fade in this experiment in a manner that depends on the length of time the cell is actually held in the deformed shape. This kind of recovery experiment for small deformations has been done before, by others (Sung et al., 1988; Dong et al., 1988), but here we repeat the experiment for larger deformations and extend the protocol to include shorter deformation/holding times.

In the second part, a theoretical model for the recovery, after large deformation, of Newtonian liquid drops is developed. The theory, which is based on a variational approach, provides a means to calculate the cell viscosity and to confirm the assumption that leukocytes behave like highly viscous liquid drops. This variational method is known as the boundary collocation method using a least squares procedure. To expedite the analyses of the experimental data, a simple procedure to obtain "closed form" or parametric solutions of the recovery problem is also described. The deformation and recovery of actual liquid drops in a viscous fluid have previously been investigated by Stone and Leal (1989). However, their numerical approach is not directly applicable to the recovery of neutrophils because it uses the boundary integral method. This method is not adequately developed for the situation in which the drop is immersed in an inviscid medium. Dong et al. (1988) have developed a theory of the recovery of a cortical shell containing a Maxwell fluid, but their theory is only valid for very small deformations. They have presented a finite element method for the large deformation of a leukocyte aspirated into a micropipette, but the problem of recovery after large deformation has not been discussed.

MATERIALS AND METHODS

Neutrophil Preparation

The methods for the preparation of cells have been described in detail elsewhere (Needham et al., 1989) and so here we will only outline the main features. The cell preparation procedure was designed to give a pure sample of neutrophils in as physiological an environment as possible, while minimizing the cells' active response to the glass surfaces of the microchamber and the pipette. Human neutrophils were isolated according to the procedure of English and Andersen (1974). Whole venous blood, anticoagulated with EDTA, was diluted to 50% (v.v.) with Ca^{2+} and Mg^{2+}-free modified Hanks' balanced salt solution (HBSS, Sigma Chemical Co., St. Louis, MO, pH 7.4, 300 mOsm) containing EDTA and carefully layered over Ficoll-Hypaque gradients (Sigma Chemical Co., Histopaque-1,077 and -1,119) having densities of 1.077 and 1.119, respectively, at 25°C. After 20 min centrifugation at 800 *g* and 25°C, the cells at the 1,077/1,119 interphase were collected and washed twice with 10× volume HBSS. The final suspension of neutrophils was in 50% autologous plasma/HBSS solution to prevent adhesion to glass surfaces (Evans and Kukan, 1984). The purity and viability of sample cells were determined by Wright stain and trypan blue exclusion tests.

Micromanipulation and Recovery

Micropipettes were made from 1-mm capillary glass tubing pulled to a fine point and broken by quick fracture to the desired tip diameter of 4.0 μm. Pipettes were filled with isosmotic buffer and were connected to a manometer via water filled tubing. Pipette pressures ranging from 10 dyn/cm^2 to 100,000 dyn/cm^2 can be applied by using the micrometer driven displacement of a water-filled reservoir or displacement of a simple suction syringe. Cells were manipulated at room temperature in a microchamber on the microscope stage by a micropipette that had been flushed previously with 50% autologous plasma solution to prevent adhesion of the cell to the glass pipette surface. Experiments were viewed with an interference contrast video microscope and recorded on video tape for subsequent geometric analysis using video calipers.

When a neutrophil is aspirated into a pipette, held within the pipette for at least a few seconds and then rapidly expelled, it slowly recovers its spherical shape. In this experiment we test the "fading memory" of the cell by monitoring recovery as a function of holding time. The pipette pressure was "zeroed," such that no flow was observed at the pipette tip. A spherical cell was identified and aspirated using a suction pressure of 5,000 dyn/cm^2. At this pressure, the cell entered the pipette in only a few seconds (Needham and Hochmuth, 1990). Upon complete entry and formation of the sausage shape, the driving pressure was immediately dropped to zero and, using gentle "mouth suction," the cell was positioned at the tip of the pipette, as shown in Fig. 2 *a*. The cell was allowed to remain in this deformed shape for a given length of time, the holding time t_h, before it was rapidly expelled into the bathing medium, as shown in Fig. 2 *b*. Close proximity to the bottom of the chamber meant that the cell would remain in the field of view while it recovered to a spherical shape without being further manipulated with a second pipette, as shown in Fig. 2, *c–e*. This absence of further micropipette manipulation also minimized cell-glass contact and helped to maintain the "passive" state of the cell during the recovery phase. With practice, the operation of positioning and expulsion could be done in 1 s. Cells were held in the deformed state for periods of time ranging from 1 to 50 s. In some cases, cells were observed to "activate" (as judged by the appearance of small protrusions and large pseudopods) while being held in the pipette or during the recovery phase. These cells were not included in the study. In the sample used for the present study, 90% of the cells were not activated.

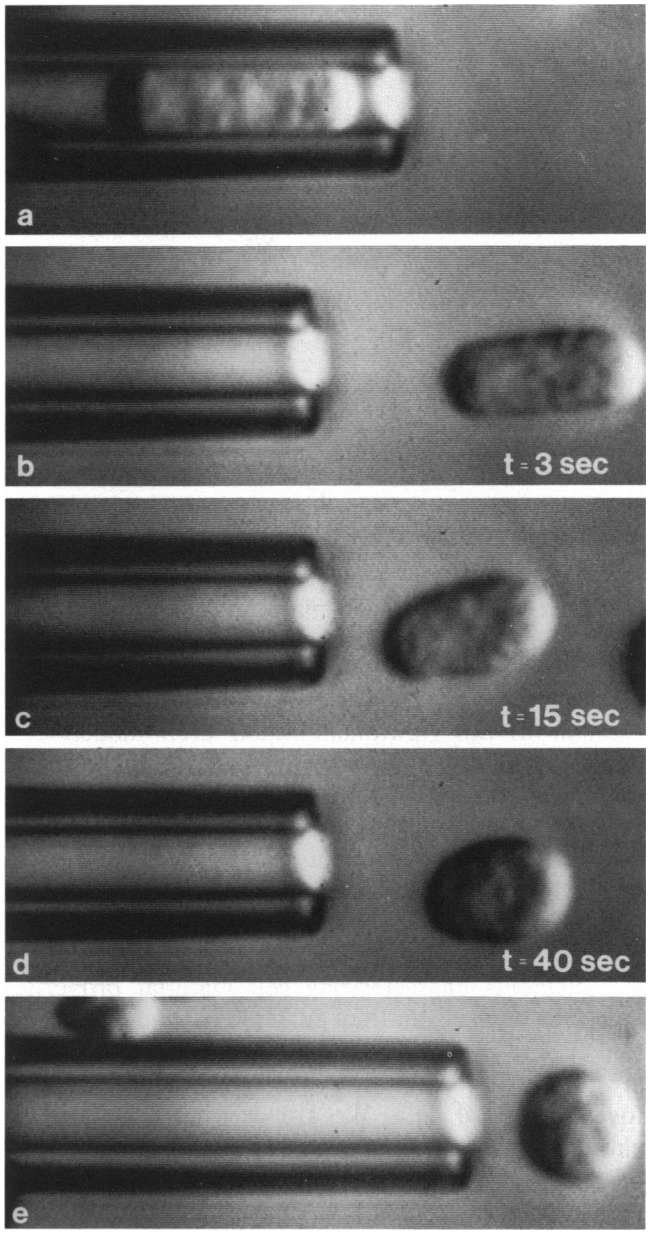

FIGURE 2 Video micrographs of recovery as a function of holding time. (**a**) A neutrophil is carefully aspirated and held in the micropipette to form relaxed sausage shape; (**b**) the cell is rapidly expelled by the application of a short positive pressure pulse and the sausage shape starts to recover. The cell is shown after expulsion at t = 3 s; (**c**) t = 15 s; and (**d**) t = 40 s. (**e**) Recovery proceeds and the cell eventually returns to its spherical shape.

EXPERIMENTAL RESULTS

Data reduction involved measuring the horizontal (D) and vertical (W) dimensions of the cell as it recovered from the deformed sausage shape to the resting spherical shape. Plots of the progress of shape recovery (D and W) versus time are shown in Fig. 3 for a cell that was held in the deformed sausage shape for 8 s and one that was held for 1.4 s. The cell that was deformed for a longer time shows a smoother recovery than the one held for the shorter time, where an initial, rapid, elasticlike recovery phase was observed. To make quantitative comparisons for the recovery of 77 cells held for a range of holding times, we measured the time required for the cell to reach 90% of its full recovery (i.e., for the cell dimension D to reach the value, $D_* = D_i - 0.9\,(D_i - D_o) = 0.1\,D_i + 0.9\,D_o$; D_i is the initial length of the deformed cell and D_o is the diameter of the resting, undeformed cell). These results as a function of holding time are shown in Fig. 4. For long holding times ($t_h > 5$ s) all the cells recovered in approximately the same time ~74 s. However, for cells held for <5 s, the cells recovered in a significantly shorter time.

THEORETICAL ANALYSIS

This analysis is for the recovery of a highly elongated axisymmetric shell like body (cortical shell) under a prestressed tension, $\overline{T}_o$, with a Newtonian fluid inside. The undeformed or reference state of the shell like body

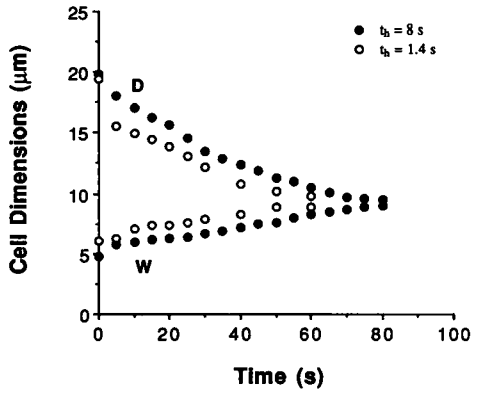

FIGURE 3 Plots of experimental data comparing the recovery of two neutrophils that were held in the pipette for 8 s and 1.4 s. Shape recovery is represented by measuring the horizontal, D, and vertical, W, dimensions of the cell versus time as it recovered from the deformed sausage shape to the resting spherical shape after the cell was expelled from the pipette.

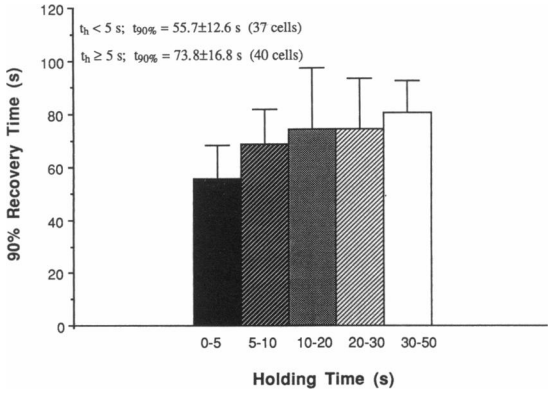

FIGURE 4 Comparison of data for 77 neutrophils and a range of holding times from 1 to 50 s. The time for the cell to reach 90% of its full recovery, (i.e., until $D = D_i - 0.9\,(D_i - D_o) = 0.1\,D_i + 0.9\,D_o$), $t_{90\%}$ is plotted against the length of time that the cell was held in the pipette t_h. D_i is the length of the elongated cell before recovery, and D_o is the diameter of the spherical cell at rest.

is assumed to be a sphere of diameter, D_o. The approach used is based on the variational method employed by Yeung and Evans (1989) for analyzing the flow of liquid like spherical cells into micropipettes. The present analysis must deal with a moving boundary, i.e., the subsequent shapes of the recovering cell are not known and have to be determined from boundary conditions that change with time.

The velocity and pressure fields inside the viscous cell are given by the general solutions to the axisymmetric creeping-flow equations and are expressed in spherical polar coordinates, R and θ, as (Haberman and Sayre, 1958; Happel and Brenner, 1986),

$$v_R(R,\theta) = -\sum_{n=2}^{\infty}(A_nR^{n-2} + C_nR^n)P_{n-1}(\cos\theta),$$

$$v_\theta(R,\theta) = \sum_{n=2}^{\infty}(nA_nR^{n-2} + (n+2)C_nR^n)\frac{I_n(\cos\theta)}{\sin\theta},$$

$$p(R,\theta) = \Pi - 2\mu\sum_{n=2}^{\infty}\left(\frac{2n+1}{n-1}\right)C_nR^{n-1}P_{n-1}(\cos\theta), \qquad (1)$$

where P_n are the Legendre polynomials and I_n are the Gegenbauer polynomials of order n given by,

$$I_n = \frac{P_{n-2} - P_n}{2n-1}. \qquad (2)$$

The parameter μ is the fluid core viscosity, and the coefficients A_n, C_n, and Π are unknowns to be determined from the boundary conditions.

The stress components in the incompressible Newto-

nian liquid core are defined as

$$\sigma_{RR} = -p + 2\mu \frac{\partial v_R}{\partial R}$$

$$\sigma_{R\theta} = \mu \left[R \frac{\partial}{\partial R}\left(\frac{v_\theta}{R}\right) + \frac{1}{R}\left(\frac{\partial v_R}{\partial \theta}\right)\right]$$

$$\sigma_{\theta\theta} = -p + 2\mu \left(\frac{1}{R}\frac{\partial v_\theta}{\partial \theta} + \frac{v_R}{R}\right). \quad (3)$$

Mechanical equilibrium for the cortical shell is given by the balance of forces, normal and tangential, to the shell contour. The cortical tension contributes only to the direction normal to the shell surface because its tangential effect cancels out. The cortical stress normal to the surface due to shell curvature is

$$\sigma_n = \overline{T}_o h, \quad (4)$$

where σ_n is the normal stress and h is the mean curvature at a point on the moving surface boundary. The equations of equilibrium in the $\hat{R}$ and $\hat{\theta}$ directions (Fig. 5) provide the stress-type boundary conditions to be satisfied:

$$\sigma_R^f + \sigma_R^c = 0,$$

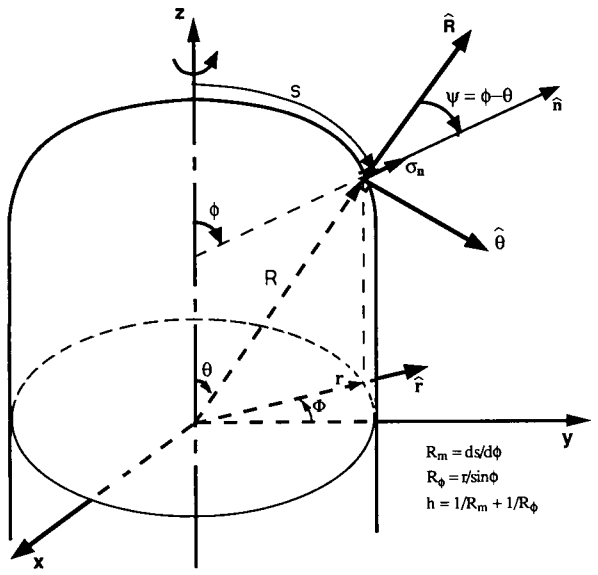

FIGURE 5 The coordinate systems used to describe an axisymmetric shell. The cartesian coordinates (x, y, z) are defined with z as the axis of symmetry; (R, θ, Φ) are the spherical coordinates; (r, Φ, z) are the cylindrical coordinates; (s, ϕ, Φ) are the curvilinear coordinates; s is the curvilinear distance; ϕ is defined as the angle that the vector, $\hat{n}$, normal to the surface makes with the z axis; σ_n is the normal component of the cortical stress; R_m and R_ϕ are the radii of curvature in the meridional and azimuthal directions, respectively; and h is the mean curvature at a point on the moving surface boundary.

and

$$\sigma_\theta^f + \sigma_\theta^c = 0, \quad (5)$$

where σ^f and σ^c are the stress components exerted at the interface by the liquid core and the cortical shell, respectively. The subscripts R and θ refer to the $\hat{R}$ and $\hat{\theta}$ directions. At the interface between the cortical shell and the liquid core, it is assumed that the velocity field is continuous. Therefore, the stress components exerted by the liquid core at the interface are obtained from the stress tensor defined in Eq. 3 by the transformation:

$$\sigma_R^f = \sigma_{RR} \cos\psi + \sigma_{R\theta} \sin\psi,$$

and

$$\sigma_\theta^f = \sigma_{R\theta} \cos\psi + \sigma_{\theta\theta} \sin\psi, \quad (6)$$

where ψ is the angle between $\hat{R}$ and the normal, $\hat{n}$, to the surface (see Fig. 5). The components of the normal cortical stress in the $\hat{R}$ and $\hat{\theta}$ directions are:

$$\sigma_R^c = \overline{T}_o \, h \cos\psi,$$

and

$$\sigma_\theta^c = \overline{T}_o \, h \sin\psi. \quad (7)$$

The solution of the recovery of a largely deformed viscous drop to its resting spherical shape due to the action of surface tension is obtained by solving the system of equations, provided by Eq. 5. However, any finite set of coefficients (A_n, C_n, and Π) will leave, in general, residual errors in the boundary conditions. Therefore, to determine the best set of coefficients and hence an approximate solution to the flow field that exactly satisfies the equations of motion in the liquid core, it is necessary to minimize the functional ϵ,

$$\epsilon = \int [(\sigma_R^f + \sigma_R^c)^2 + (\sigma_\theta^f + \sigma_\theta^c)^2] \, r \, ds, \quad (8)$$

which is a measure of these errors over the surface of the shell (Fig. 5). Differentiation of the functional with respect to each coefficient leads to a system of linear equations, $\partial\epsilon/\partial a_i$, that can be easily solved,

$$\frac{\partial \epsilon}{\partial a_i} = 2 \int \left[(\sigma_R^f + \sigma_R^c) \frac{\partial \sigma_R^f}{\partial a_i} + (\sigma_\theta^f + \sigma_\theta^c) \frac{\partial \sigma_\theta^f}{\partial a_i} \right] r ds = 0, \quad (9)$$

where the variables, a_i, refer to the coefficients Π, A_n, and C_n.

A stepwise procedure is used to compute the shape recovery. From the shape of the cell at time, t, the cortex velocity field is calculated from Eq. 1 in which the unknown coefficients are determined from Eq. 9. The shape of the cell at time, $t + dt$, is then computed from its shape at time, t. From this new shape, the cortex

velocity is calculated, and so on. The new shape of the cell is determined in the $r - z$ plane (Fig. 5) by the equations

$$r = r_t + v_r\, dt,$$

and

$$z = z_t + v_z\, dt, \tag{10}$$

where r and z are the coordinates at time $t + dt$ in the $\hat{r}$ and $\hat{z}$ directions, respectively, whereas r_t and z_t are the corresponding coordinates at time t. (The shape of the deformed shell at zero time is assumed to be known). The shell velocities, at time t, in the cylindrical coordinate system (r, Φ, z) are given by

$$v_r = v_R \sin\theta + v_\theta \cos\theta,$$

and

$$v_z = v_R \cos\theta - v_\theta \sin\theta. \tag{11}$$

The two dimensions of interest are the length, D, and width, W, of the shell because they are the known experimental parameters. These dimensions correspond to the size of the cell along the axes $z = 0$ and $r = 0$, respectively.

EQUATIONS FOR SHAPE RECOVERY

Because the recovery process strongly depnds on the initial degree of deformation, any solution that does not explicitly give the deformed length, D, and width, W, of the drop as a function of the initial cell dimensions before recovery and as a function of time is not suitable for covering a wide, continuous range of deformations. Therefore, to be able to analyze a large number of liquid drops or cells of different size, the solutions, (i.e., D/D_o and W/D_o), must be expressed as a function of the initial deformation ratio, D_i/D_o or W_i/D_o, and the dimensionless time, $\bar{t} = t\,\bar{T}_o/\mu R_o$. Time is scaled with respect to the radius, R_o, of the undeformed drop or cell ($R_o = D_o/2$).

In this section, the main steps used to transform the numerical solutions described above into parametric solutions are outlined. First, we must note that the theoretical length and width of the cell, as recovery proceeds, can be expressed as

$$\frac{L}{D_o} = \frac{L_i}{D_o} + A\bar{t} + B(\bar{t})^2 + C(\bar{t})^3 + \ldots, \tag{12}$$

where L represents the length, D, or width, W, of the deformed drop or cell, and the subscript i refers to the initial value before recovery. The coefficients in the polynomial are functions of the ratio, L_i/D_o. The initial deformation index is defined as the ratio D_i/D_o.

$$A = A_o + A_1(L_i/D_o) + A_2(L_i/D_o)^2 + A_3(L_i/D_o)^3 + \ldots,$$
$$B = B_o + B_1(L_i/D_o) + B_2(L_i/D_o)^2 + B_3(L_i/D_o)^3 + \ldots,$$
$$C = C_o + C_i(L_i/D_o) + C_2(L_i/D_o)^2 + C_3(L_i/D_o)^3 + \ldots,$$
etc. (13)

For the special case where $L_i/D_o \to 1$, i.e., in the resting state, the above coefficients must satisfy the constraint:

$$A_o + A_1 + A_2 + A_3 + \ldots = 0,$$
$$B_o + B_1 + B_2 + B_3 + \ldots = 0,$$
$$C_o + C_1 + C_2 + C_3 + \ldots = 0,$$
etc. (14)

From the analysis described in the previous section, it is found that for $(D_i/D_o) \leq 3.5$ and $\bar{t} \leq 3.5$, the length and width of a recovering cell can be approximated by polynomials of third order:

$$\frac{D}{D_o} = \frac{D_i}{D_o} + A\bar{t} + B(\bar{t})^2 + C(\bar{t})^3;$$
$$\frac{W}{D_o} = \frac{W_i}{D_o} + D\bar{t} + E(\bar{t})^2 + F(\bar{t})^3. \tag{15}$$

The upper limit for the index of deformation is chosen to cover the range of deformations found in our experiments.

The procedure to derive the unknown coefficients appearing in the above approximate solutions is as follows. First, a series of values for the coefficients A–F is generated as a function of D_i/D_o or W_i/D_o. This is done by fitting Eq. 15 to the dimensionless values of length and width given by the theory for a series of deformations, (D_i/D_o), ranging from 1.1 to 3.5. Next, a curve fitting of the generated discrete values is performed for each of the coefficients A–F using Eqs. 13 and 14. These unknown coefficients are then found to have the form

$$A = A_o + A_1(D_i/D_o),$$
$$B = B_o + B_1(D_i/D_o),$$
$$C = C_o + C_1(D_i/D_o) + C_2(D_i/D_o)^2, \tag{16}$$

and

$$D = D_o + D_1(W_i/D_o) + D_2(W_i/D_o)^2 + D_3(W_i/D_o)^3,$$
$$E = E_o + E_1(W_i/D_o) + E_2(W_i/D_o)^2 + E_3(W_i/D_o)^3 + E_4(W_i/D_o)^4,$$
$$F = F_o + F_1(W_i/D_o) + F_2(W_i/D_o)^2 + F_3(W_i/D_o)^3 + F_4(W_i/D_o)^4. \tag{17}$$

The coefficients, $A_o - F_4$, appearing in Eqs. 16 and 17 are equal to

$$A_o = -A_1 = 0.71380;$$
$$B_o = -B_1 = -0.17426;$$
$$C_o = 0.017446, C_1 = -0.018588, C_2 = 0.001142; \quad (18)$$

and

$$D_o = -0.05222, D_1 = 0.59809, D_2 = 0.13979, D_3 = -0.68566;$$
$$E_o = 0.09739, E_1 = -0.19123, E_2 = -0.14642, E_3 = 0.02089, E_4 = 0.21937;$$
$$F_o = -0.015683, F_1 = 0.024884, F_2 = 0.020053, F_3 = -0.001595, F_4 = -0.027659. \quad (19)$$

Therefore, the recovery of a liquid drop from an initially deformed sausage shape is completely determined by Eqs. 15–19, once the index of deformation is specified. This finding is very useful because one does not have to use the general complex theory. The approximate solutions (i.e., Eqs. 15–19) then provide a means to expedite the analyses of the experimental data. Theoretical values for the length and width of the cell can be calculated with respect to the dimensionless time and compared to experimental values. A computer program is written to give the best fit, i.e., the optimal ratio T_o/μ, to the experimental values of D/D_o and W/D_o. It should be emphasized that these parametric solutions are valid only for $(D_i/D_o) \leq 3.5$ and $\bar{t} \leq 3.5$.

THEORETICAL RESULTS

In the numerical computation, the contour of half of the shell was decomposed into 61 equally spaced nodes, and 58 terms were used in the summation (Eq. 1). A small time step was used to compute the subsequent shapes. This step size was selected to satisfy both the condition of symmetry about the r-axis and the constraint of constant volume. (A more elongated shell requires a smaller time step because the speed of the shell motion is faster).

A typical recovery is shown in Fig. 6, where the computed shapes are plotted as a function of a dimensionless time. For computational purposes, this time is scaled by the length of the major semi-axis of the initial deformed sausage shape, $R_i(R_i = D_i/2)$. The index of deformation, D_i/D_o, for this particular shell is two. The theory generates a series of recovery profiles starting from the deformed sausage shape and ending up with a

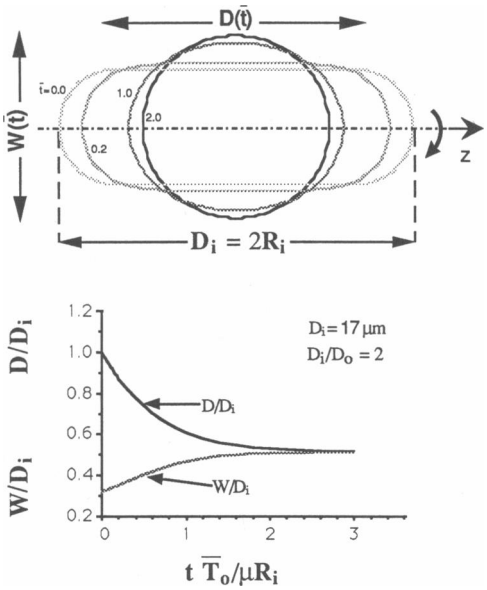

FIGURE 6 A series of recovery profiles starting from the deformed sausage shape and ending up with a sphere are generated from the theory. Below these recovery profiles is shown the dimensionless plot of the corresponding length and width of the shell. For computation purposes, this dimensionless time is scaled by the initial length of the semi-axis of the elongated shell.

sphere. The corresponding dimensionless length and width are shown, below the recovery profiles, as a function of the same dimensionless time.

Very good agreement is found between the approximate (Eqs. 15–19) and numerical solutions for $1.1 < D_i/D_o < 3.5$ and $\bar{t} < 3.5$ (Fig. 7). For clarity, only the results for the two extreme and mid values of the selected range of deformations are shown. The good fit between the two analyses deteriorates as the cell becomes more elongated. If the deformation is too large (i.e., for outside the limit $D_i/D_o > 3.5$), the exact theory must be used or a new set of coefficients (Eqs. 16–19) needs to be determined. Because the results predicted by the approximate and numerical solutions are comparable in the range of deformations performed, the parametric solutions are used to analyze the experimental data. The advantage of these solutions (third order polynomials) is that the length, L, and width, W, of a cell, as it recovers its spherical shape, are completely determined by specifying only the initial cell dimensions, (i.e., D_i/D_o and W_i/D_o). These dimensions, L and W, are then functions of the dimensionless time $\bar{t}$ only. For practical reasons, the dimensionless time and the cell lengths are scaled with respect to R_o and D_o, respectively.

Fig. 8 shows the theoretical fit to the recovery for a neutrophil that has been held in the deformed sausage shape inside the pipette for 8 s. The ratio of cortical

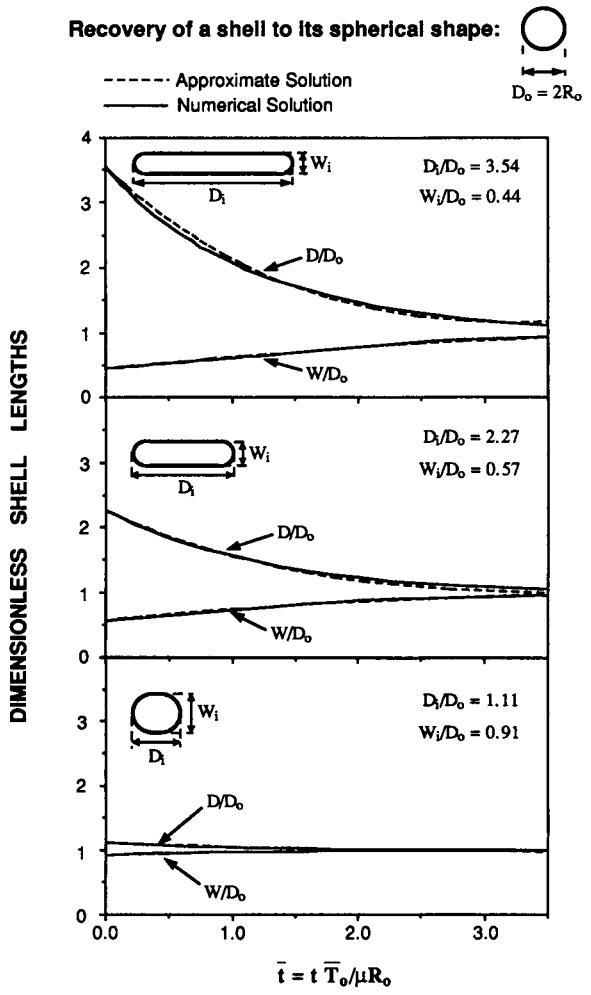

FIGURE 7 Comparison of the results given by the approximate (i.e., Eqs. 15–19) and numerical solutions. For practical purposes, the dimensions of the elongated cell are scaled by the diameter of its resting spherical shape. The recovery of these dimensionless lengths are shown as a function of the dimensionless time, $\bar{t}$, for three initial deformation indices (i.e., D_i/D_o = 3.5, 2.3, and 1.1). This figure also shows the corresponding initial shapes the spherical shell (given at the top of the figure) must take. In the drawings of the different shapes, the length scale is preserved (i.e., the volume of the sketched deformed sausagelike shells is equal to the volume of the sketched spherical shell).

tension to cytoplasmic viscosity $\bar{T}_o/\mu$ is the fitting parameter. The best fit of the Newtonian theory to the experimental data gives a value for $\bar{T}_o/\mu$ of 1.83×10^{-5} cm/s. This particular cell has an initially deformed sausagelike shape with a deformation index, D_i/D_o, of 2.3. The dimensionless lengths are given as a function of the dimensionless time, $\bar{t}$. As seen, excellent agreement is found between the theory and experiments and confirm earlier reports (Yeung and Evans, 1989; Evans and Yeung, 1989; Needham and Hochmuth, 1990) that,

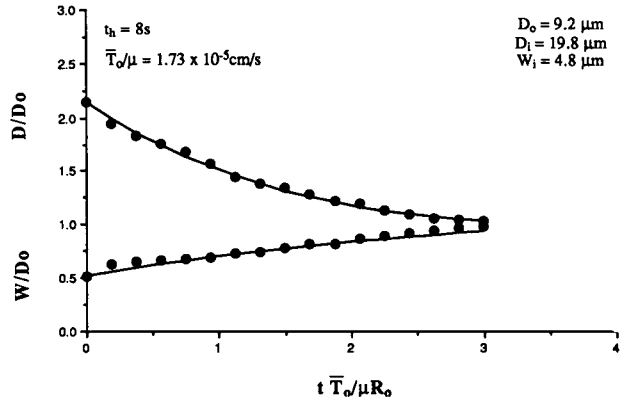

FIGURE 8 Dimensionless plots showing the best fit of the Newtonian model to the experimental data shown in Fig. 3, t_h = 8 s. The apparent viscosity derived from this fit is 2,023 poise and 1,156 poise, when assuming a constant cortical tension of 0.035 dyn/cm and 0.024 dyn/cm, respectively.

even though the cell interior consists of a complex matrix, passive neutrophils behave like Newtonian liquid drops under certain experimental conditions. It is important to note that if the cell interior is a Maxwell liquid, the exact same recovery profile will be obtained if the spring element is fully relaxed, i.e., if the cell is held in the deformed state long enough for the actin network to relax. Otherwise, an initial elastic recoil will be seen at the time when the cell starts its recovery immediately after expulsion from the holding pipette. This is the

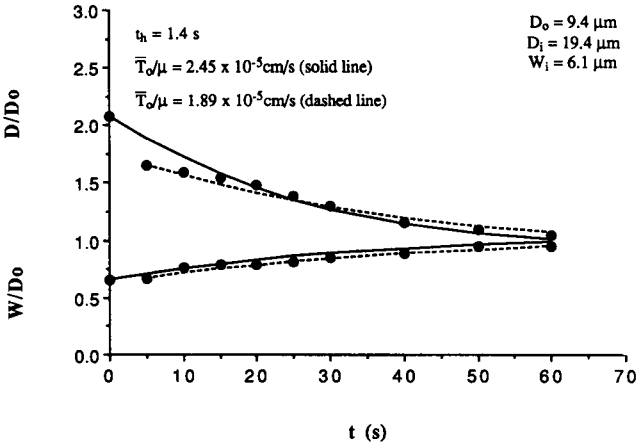

FIGURE 9 Plots showing the best fits of the Newtonian model to the experimental data shown in Fig. 3, t_h = 1.4 s. The apparent viscosity derived from these data (*solid line*) is 1,426 poise and 815 poise, when assuming a constant cortical tension of 0.035 dyn/cm and 0.024 dyn/cm, respectively. When the data for $t \leq 5$ s are excluded from the analysis, a value of 1,852 poise and 1,058 poise is obtained, respectively.

reason that for short holding times the best fit of the Newtonian theory to the experimental data is not satisfactory as shown in Fig. 9. For a holding time $t_h > 5$ s the average value for $\overline{T}_o/\mu$ is $1.7 \pm 0.5 \times 10^{-5}$ cm/s, whereas for $t_h < 5$ s the average value for $\overline{T}_o/\mu$ is $2.6 \pm 0.8 \times 10^{-5}$ cm/s (Fig. 10). The larger average value for $\overline{T}_o/\mu$ is a consequence of the elastic recoil. The experimental data for short holding times must therefore be analyzed with a viscoelastic liquid model, the simplest of these models is the Maxwell liquid.

The validity of the present theory has been verified by recovery experiments performed on Newtonian drops in deionized water. The Newtonian drops used in these experiments are silicone oil drops with known surface tension and viscosity. Very good agreement is found between the values for $\overline{T}_o/\mu$ predicted by the theory and the exact ones (Fig. 11). The theory gives a value of 0.415 ± 0.017 cm/s and the measurements a value of 0.432 ± 0.009 cm/s. The surface tension between deionized water and silicone oil as determined by the drop weight method was 45.4 ± 0.4 dyn/cm, and the viscosity of the oil as measured with a Cannon-Fenske viscometer was 105.0 ± 0.1 poise.

DISCUSSION

In the search for the parametric solutions to the recovery problem, an upper limit of 3.5 is set for the deformation D_i/D_o, which corresponds to a dimensionless width W_i/D_o of 0.4 because volume is conserved. The shape of a deformed cell with an index of 3.5 is shown in Fig. 7. As can be seen, the cell is quite elongated at this degree of deformation. The actual limit for this kind of spherical to "sausage" shape deformation for a neutrophil is determined by the amount of excess membrane area that can be unravelled from membrane ruffles before a static limit is reached. Further area dilation results in cell lysis. This area limit is ~110%–120% of the area of the undeformed spherical cell, and corresponds to the deformation of a neutrophil into a 2.7-μm diameter pipette (Evans and Yeung, 1989). The largest deformation performed in our deformation – recovery analysis is comfortably inside this limit. In the present experiments, the cells are aspirated into 4-μm diameter pipettes. A deformation ratio D_i/D_o of 3.5 represents a 56% area expansion of the ruffle membrane.

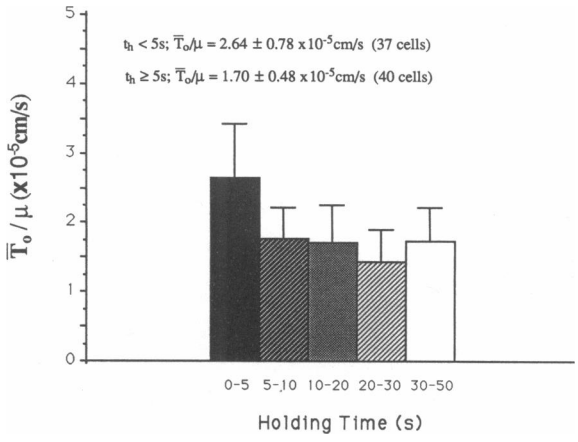

FIGURE 10 Best fit parameter $\overline{T}_o/\mu$ as a function of holding time. Based upon the assumption of a constant cortical tension of 0.035 dyn/cm and 0.024 dyn/cm, the average viscosity is, respectively, 2,212 ± 581 poise and 1,517 ± 398 poise, for $t_h > 5$ seconds. For $t_h < 5$ s, the apparent viscosity is significantly smaller due to the elastic recoil, and is 1,438 ± 419 poise and 986 ± 287 poise, respectively.

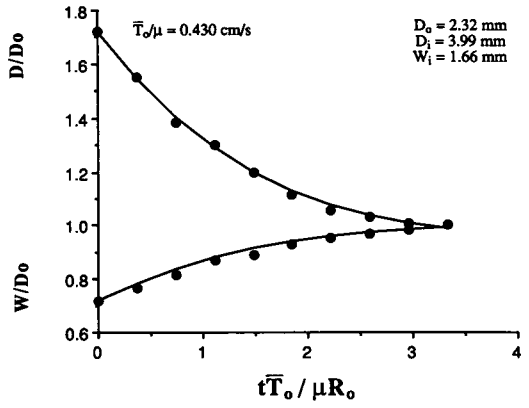

FIGURE 11 Recovery of a silicone oil drop in deionized water. Independent measurements of the surface tension and oil viscosity give a ratio $\overline{T}_o/\mu$ of 0.432 ± 0.009 cm/s. The theory gives a mean value of 0.415 ± 0.017 cm/s.

From the ratio $\overline{T}_o/\mu$, we would like to extract information regarding cell mechanical properties. In the present recovery experiment, it is not possible to extract an exact value for μ without a precise knowledge of the value for $\overline{T}_o$. We have recently found that $\overline{T}_o$ has a mean value of 0.024 dyn/cm (unpublished data) which yields an average value for the viscosity of 1,517 ± 398 poise, as long as the cells are held in the pipette for >5 s. This value compares very well with the viscosity value of 1,350 ± 540 poise determined from experiments involving pipette entry and flow of passive neutrophils from the same donors (Needham and Hochmuth, 1990). In other studies, a constant value for $\overline{T}_o$ of 0.035 dyn/cm has been found (Evans and Yeung, 1989) which, for comparison, gives an average value for the viscosity of 2,212 ± 581 poise. Evans and Yeung have reported a value for the

viscosity of 2,100 ± 1,000 poise. The general agreement in the calculated values for the cytoplasmic viscosity between the present experiments and those of pipette entry and flow gives additional support to the model of the neutrophil as a highly viscous Newtonian liquid drop with a persistent cortical tension. However, in both experiments, certain features point to more complex behavior for small deformations, for high rates of deformation, and for short holding times before recovery is allowed to proceed. A "jump-in" is observed in the plots of L_p (the instantaneous projection length of the cell in the pipette) versus time for the initial phase of entry of the cell into the pipette (Needham and Hochmuth, 1990). The "jump-in" is larger for higher excess suction pressures and concomitantly higher rates of deformation. This instantaneous projection length is observed to be larger than the radius of the pipette, R_p, at zero time. However, a Newtonian liquid drop model allows no instantaneous deformation at zero time. Thus, we attribute this behavior to an elastic response of the cytoplasm.

A viscoelastic behavior is also observed in our recovery experiments when the deformation and holding times are less than 5 s. When a cell is rapidly aspirated into a parallel pipette and expelled as fast as possible (total deformation time ~1 s) the cell shows an asymmetric recovery. The front part of the cell that entered the pipette first and exited last was deformed for a slightly longer time than the back half of the cell. This asymmetry in recovery, within the same cell, clearly indicates that some interior elastic element is operating that influences the recovery behavior. This influence depends on how rapidly the elastic element is loaded and how long it is allowed to relax before the cell is allowed to recover. For such rapid deformations and holding times less than ~5 s the recovery profile is not that of a Newtonian liquid as shown in Fig. 9. Attempts to fit the whole recovery with a Newtonian theory clearly fail, although after the initial recoil the remaining recovery can be fit with the Newtonian liquid drop model as shown by the dashed curve in Fig. 9. When the initial recoil is excluded from the curve fitting, the values for $\overline{T}_o/\mu$ obtained for the cells held for short times are in agreement with those in which cells were held for relatively long times. For progressively longer holding times the spring can relax as strain is transferred to the viscous element until all "fading memory" is lost for holding times > ~5 s, Fig. 8. Thus, the response of the cell to initial, rapid deformations and short holding times show that the Newtonian liquid element must be replaced by a Maxwell liquid element. We are currently incorporating this into our analyses for large rapid deformations.

In summary, the boundary collocation method using least squares procedure is applied to the recovery of a prestressed spherical thin shell containing a Newtonian liquid after large axisymmetric deformation. It is found that recovery experiments can be analyzed over a wide range of strains by using for the major and minor lengths a set of third order polynomials that depend only on the deformation ratio, D_i/D_o or W_i/D_o, and the dimensionless time, $\bar{t} = t\,\overline{T}_o/\mu R_o$. These findings are important because they allow one to analyze large quantities of recovery data in terms of the cell mechanical properties. Finally, it is also found that passive neutrophils behave as Newtonian liquid drops during recovery as long as the cells are held in the pipette for >5 s. Under this condition, the ratio of cortical tension to cytoplasmic viscosity, $\overline{T}_o/\mu$, is in the order of 1.7×10^{-5} cm/s.

Although the analysis described here is restricted to a Newtonian liquid core, the variational method presented can be extended to more complex situations, e.g., where the cell core and/or the cortex have viscoelastic properties.

This work was supported by the National Institutes of Health grant 2R01-HL-23728.

Received for publication 22 March 1991 and in final form 21 June 1991.

REFERENCES

Bagge, U., R. Skalak, and R. Attefors. 1977. Granulocyte rheology: experimental studies in an in-vitro microflow system. *Adv. Microcirc.* 7:29–48.

Dong, C., R. Skalak, K. L. P. Sung, G. W. Schmid-Schönbein, and S. Chien. 1988. Passive deformation analysis of human leukocytes. *J. Biomech. Eng.* 110:27–36.

English, D., and B. R. Andersen. 1974. Single step separation of red blood cells, granulocytes and mononuclear leukocytes on discontinuous density gradients of ficoll-hypaque. *J. Immunol. Methods.* 5:249–252.

Evans, E. A. 1984. Structural model for passive granulocyte based on mechanical deformation and recovery after deformation test. *In* White Cell Mechanics: Basic Science and Clinical Aspects. H. J. Meiselman, M. A. Lichtman, and P. L. LaCelle, editors. Alan R. Liss, Inc., New York, 53–74.

Evans, E. A., and B. Kukan. 1984. Passive behavior of granulocytes based on large deformation and recovery after deformation tests. *Blood.* 64:1028–1035.

Evans, E. A., and A. Yeung. 1989. Apparent viscosity and cortical tension of blood granulocytes determined by micropipet aspiration. *Biophys. J.* 56:151–160.

Haberman, W. L., and R. M. Sayre. 1958. Motion of rigid and fluid

spheres in stationary and moving liquids inside cylindrical tubes. Department of the Navy, David Taylor Model Basin. Hydromechanics Laboratory, Research and Development Report, 1143.

Happel, J., and H. Brenner. 1986. Mechanics of Fluids and Transport Processes. Low Reynolds Number Hydrodynamics. Martinus Nijhoff Publishers. Boston, Massachusetts.

Needham, D., M. Armstrong, R. S. Nunn, and D. L. Hatchell. 1989. Rapid deformation of "passive" polymorphonuclear leukocytes: the effects of pentoxifylline. *J. Cell Physiol.* 140:549–557.

Needham, D., and R. M. Hochmuth. 1990. Rapid flow of passive neutrophils into a 4-μm pipette and measurement of cytoplasmic viscosity. *J. Biomech. Eng.* 112:269–276.

Schmid-Schönbein, G. W., K.-L.P. Sung, H. Tözeren, R. Skalak, and S. Chien. 1981. Passive mechanical properties of human leukocytes. *Biophys. J.* 36:243–256.

Stone, H. A., and L. G. Leal. 1989. Relaxation and breakup of an initially extended drop in an otherwise quiescent fluid. *J. Fluid Mech.* 198:399–427.

Sung, K.-L.P., C. Dong, G. W. Schmid-Schönbein, S. Chien, and R. Skalak. 1988. Leukocyte relaxation properties. *Biophys. J.* 54:331–336.

Yeung, A., and E. A. Evans. 1989. Cortical shell-liquid core model for passive flow of liquid-like spherical cells into micropipets. *Biophys. J.* 56:139–149.